AGU PUBLICATIONS

JGR

Journal of Geophysical Research: Space Physics

RESEARCH ARTICLE

10.1002/2016JA023076

Upper limit of electron fluxes generated by kinetic Alfvén waves in Maxwellian plasma

A. V. Artemyev[1,2], R. Rankin[3], and I. Y. Vasko[2,4]

[1]Institute of Geophysics and Planetary Physics, University of California, Los Angeles, California, USA, [2]Space Research Institute, RAS, Moscow, Russia, [3]Department of Physics, University of Alberta, Edmonton, Alberta, Canada, [4]Space Science Laboratory, University of California, Berkeley, USA

Key Points:
- Electron acceleration by kinetic Alfvén waves in the equatorial inner magnetosphere and plasma sheet boundary layer
- Energy variations of trapped and transient resonant electrons almost compensate each other
- Kinetic Alfvén waves accelerate trapped electrons without being significantly damped

Correspondence to:
A. V. Artemyev,
aartemyev@igpp.ucla.edu

Citation:
Artemyev, A. V., R. Rankin, and I. Y. Vasko (2016), Upper limit of electron fluxes generated by kinetic Alfvén waves in Maxwellian plasma, *J. Geophys. Res. Space Physics*, *121*, 8361–8373, doi:10.1002/2016JA023076.

Received 16 JUN 2016
Accepted 17 AUG 2016
Accepted article online 22 AUG 2016
Published online 5 SEP 2016

Abstract We consider electron acceleration by kinetic Alfvén waves in the equatorial inner magnetosphere and plasma sheet boundary layer. The competition between the accelerating effect of the wave parallel electric field and mirror force acting on particles in an inhomogeneous background magnetic field generates an effective potential well where electrons can be trapped and accelerated. We compare energy variations of trapped and transient resonant electrons and show that these variations almost compensate each other. Thus, energy provided to waves by transient particles is transferred to trapped particles. This effect allows waves accelerate trapped electrons without being significantly damped. Using energy balance equations, we estimate the maximum flux of electrons accelerated via trapping into Landau resonance with kinetic Alfvén waves. For a wide range of system parameters (i.e., ion to electron temperature ratio, magnetic field amplitude, and wave number and wave frequency), acceleration of trapped electrons can generate fluxes with amplitude about 5–25% of the background thermal fluxes. We determine parametric regions for the most efficient acceleration.

1. Introduction

A critical aspect of the generation of aurora at high latitudes is acceleration of cold (10–100 eV) electrons up to keV energies along magnetic field lines. One of the most promising acceleration mechanisms relates to the parallel electric field of kinetic Alfvén waves (KAWs) that are widely observed near the plasma sheet boundary layer [e.g., *Wygant et al.*, 2002] and in the equatorial inner magnetosphere [e.g., *Chaston*, 2015; *Ergun et al.*, 2015, and references therein]. A generation mechanism for KAWs with transverse wavelength about the ion gyroradius is recently proposed by *Zhao et al.* [2014], whereas KAWs with higher wave frequency can be naturally produced through the turbulent cascade mechanism [*Zhao et al.*, 2016]. Electron interaction with wave electric fields includes both reflection [*Kletzing*, 1994] and trapping [*Hasegawa*, 1976] of particles. Moreover, natural inhomogeneity of the background plasma density and magnetic field B significantly modifies these mechanisms of wave-particle interaction (see review by *Shklyar and Matsumoto* [2009, and references therein]).

The frequency of KAWs, ω, is lower than the ion gyrofrequency and much lower than the electron gyrofrequency; thus, only Landau resonance can be considered for thermal electron interaction with KAWs: $k_{||}v_{||}=\omega$ (where $k_{||}$ is a parallel wave vector and $v_{||}$ is the parallel component of electron velocity). This resonance does not perturb the first adiabatic invariant (magnetic moment, μ). Therefore, the total energy of trapped particles moving with the wave can be expressed as a sum of parallel $\sim m_e(\omega/k_{||})^2/2$ and transverse μB energy components [*Artemyev et al.*, 2015a], where m_e is the electron mass. Thus, particle acceleration is due to the growth of the wave phase velocity $\omega/k_{||}$ along magnetic field lines [*Laval and Pellat*, 1970; *Karpman and Shklyar*, 1972] and the increase of the background magnetic field intensity B [*Nunn*, 1971; *Karpman and Shklyar*, 1975]. Gradients of B and $k_{||}$ contribute to an effective mirror force [e.g., *Artemyev et al.*, 2012] acting on particles in resonance with KAWs. The balance between this force and the force of the wave parallel electric field generates potential well for particle trapping. Thus, the trapping mechanism is based on system inhomogeneity and differs from the trapping into the wave potential [*Hasegawa*, 1976]. The natural limitation of this trapping corresponds to the amplitude of the parallel electric field: when KAWs with trapped particles reach a region with strong enough gradients of B and $k_{||}$, the wave electric field cannot counterbalance the effective mirror force, and particles escape from the resonance region. Thus, to transport trapped electrons at high-enough

magnetic latitudes (e.g., to reach the aurora region), the amplitude of the parallel electric field should be sufficiently strong. Moreover, the same wave amplitude defines the maximum possible energy gained by particles trapped into Landau resonance [*Artemyev et al.*, 2012].

Due to the relatively long parallel wavelength of KAWs, the wave scalar potential Φ_0 is large, and the corresponding width of the resonance region in velocity space $\sim \sqrt{e\Phi_0 m_e}$ [*Karney*, 1978] is wide enough to trap a significant number of particles (the corresponding resonance width in energy space is $\sim\sqrt{e\Phi_0 m_e}(\omega/k_\parallel)$). Thus, if energy for trapped particle acceleration is provided by waves, rapid wave damping should occur. However, in an inhomogeneous magnetic field there is another mechanism of energy exchange between transient particles scattered by waves and trapped particles [*Karpman et al.*, 1975; *Shklyar*, 2011] in which waves play a role of mediator between two particle populations. In this case, waves can survive for a long time and provide an effective acceleration of trapped population.

The effect of electron trapping by KAWs in inhomogeneous plasma was modeled by *Watt and Rankin* [2009, 2010] and explained analytically by *Artemyev et al.* [2015a]. However, analytical estimates were performed for an overestimated amplitude of the scalar potential without taking into account effects of wave damping/amplification. Moreover, previous estimates were made for a narrow range of background parameters (such as plasma density, temperature of ions and electrons, and wave characteristics). As shown by *Damiano et al.* [2015], the relative amplitude of the KAW parallel electric field is very sensitive to the background plasma parameters (e.g., ion temperature). Thus, in this paper we perform a parametric study of the trapping mechanism of electron acceleration by KAWs. We consider contributions of transient and trapped particles to estimate an upper limit of accelerated electron fluxes generated by KAWs. All calculations are shown for two plasma regions: the equatorial inner magnetosphere and plasma sheet boundary layer.

2. Electron Resonant Interaction With KAW

We consider the resonant interaction of nonrelativistic electrons (charge $-e$, mass m_e) with KAWs propagating obliquely to the background magnetic field. The wave frequency ω is less than the ion (and much less than electron) gyrofrequency. This condition excludes from consideration all cyclotron resonances and leaves only Landau resonance $k_\parallel v_\parallel = \omega$.

In the equatorial magnetosphere and plasma sheet boundary layer the Landau resonance condition is satisfied for electrons with temperatures on the order of tens to hundreds of eVs. If we exclude cyclotron resonances, the electron magnetic moment $\mu = m_e v_\perp^2/2B$ is conserved (B is background magnetic field magnitude and $v_\perp$ is the electron transverse component of velocity). Conservation of magnetic moment allows us to consider only electron motion along magnetic field lines [*Northrop*, 1963; *Sivukhin*, 1965] with the corresponding Hamiltonian

$$H = \frac{p^2}{2m_e} + \mu B(s) - e\Phi(s,t) \tag{1}$$

where $p = m_e v_\parallel$ is the electron parallel momentum, s is a coordinate along magnetic field lines, and $\Phi(s,t)$ is the potential of KAWs (we consider transverse wavelength much larger than electron gyroradius). Potential Φ is defined in a such way, which gradient $\partial\Phi/\partial s$ gives the wave parallel electric field including both potential and induction fields, i.e., Φ is an effective potential describing both electric field corresponding to scalar and vector potentials of KAWs [see, e.g, *Artemyev et al.*, 2015a, Appendix, and references therein]. We assume that $\Phi = \tilde{\Phi}(s)F(\psi)$ where $\tilde{\Phi}(s)$ is the effective amplitude of the scalar potential, function $F(\psi)$ determines the wave packet shape, and ψ is the wave phase (ψ_0 is the initial phase):

$$\psi = \psi_0 + \int_{s_0}^{s} k_\parallel(\tilde{s})\mathrm{d}\tilde{s} - \omega t \tag{2}$$

where s_0 is coordinate of wave generation region. The model used to define $\tilde{\Phi}(s)$ and $k_\parallel$ is described in Appendix A. It shows that we can write $\tilde{\Phi} = \Phi_0 w(s)$ and $k_\parallel = k_0 K(s)$ with functions $w(s)$, $K(s)$ given by equations (A5) and (A6). We introduce the dimensionless coordinate $z = s/R$ (where R is a typical spatial scale of inhomogeneity of the background magnetic field), momentum $p_z = p/m_e v_{A0}$ (where v_{A0} is the Alfvén velocity defined in the region of KAW generation), magnetic field $b = B/B_0$ (where B_0 is an background magnetic field in the region of KAW generation), wave amplitude $\phi_0 = e\Phi_0/m_e v_{A0}^2$, magnetic moment $\mu^* = 2\mu B_0/m_e v_{A0}^2$, parameter $\chi = \omega R/v_{A0}$ (note that the definition of k_0 gives $k_0 v_{A0}/\omega = 1$, see Appendix A). Through the paper,

we consider $\chi \gg 1$, i.e., parallel wavelength $\sim v_{A0}/\omega$ is much smaller than a scale of magnetic field inhomogeneity, R. This condition allows us to describe processes of electron acceleration and energy exchange between different electron populations analytically. However, it excludes from the consideration waves that have parallel wavelengths comparable to the length of the field line (e.g., field line resonances). For systems with $\chi \sim 1$, timescales of the wave-particle resonant interaction and the wavefield evolution are not separated [*Rankin et al.*, 1999; *Tikhonchuk and Rankin*, 2002], and thus, another approach should be used.

In new variables, the normalized Hamiltonian ($H \to H/m_e v_{A0}^2$) and phase (1), (2) take the form

$$\begin{aligned} H &= \frac{1}{2}p_z^2 + \frac{1}{2}\mu^* b(z) - \phi_0 w(z) F(\psi) \\ \psi &= \psi_0 + \chi\left(\int_{z_0}^{z} K(\tilde{z})\mathrm{d}\tilde{z} - t\right). \end{aligned} \tag{3}$$

Due to $\chi \gg 1$, i.e., system (3) describes evolution of slow variables (z, p_z) and fast phase ψ. The Hamiltonian equations for Hamiltonian (3) can be written as

$$\dot{z} = \frac{\partial H}{\partial p_z} = p_z, \quad \dot{p}_z = -\frac{\partial H}{\partial z} = -\frac{1}{2}\mu^* b' + \phi_0 w' F + \chi\phi_0 K w F' \tag{4}$$

where $'$ denotes the derivative relative to the argument of the corresponding function. Using equations $\dot{\psi} = \chi(K\dot{z} - 1)$ and $\ddot{\psi} = \chi(K\ddot{z} + K'\dot{z}^2)$, we can rewrite equation (4) as

$$\frac{\ddot{\psi}}{\chi} = -\frac{1}{2}\mu^* K b' + K'\dot{z}^2 + K\phi_0\left(w'F + \chi K w F'\right). \tag{5}$$

We can omit the term $\sim w'$ because $\chi \gg 1$ and $w'F \ll \chi K w F'$. Near the resonance location $\dot{\psi} = 0$ we have $\dot{z} = p_z = 1/K$:

$$\frac{\ddot{\psi}}{\chi} = -\frac{1}{2}\mu^* K b' + K' K^{-2} + \phi_0 \chi K^2 w F'. \tag{6}$$

Taking into account that phase ψ changes much faster than coordinate z, we can consider z as a parameter and write the Hamiltonian for equation (6):

$$H_\psi = \frac{1}{2}\chi^2 K^2 p_\psi^2 + \frac{1}{2}\frac{1}{\chi K}\left(\mu^* b' + (K^{-2})'\right)\psi - \phi_0 w F(\psi) \tag{7}$$

where $(K^{-2})' = -2K'/K^3$, and $p_\psi = \dot{\psi}/(\chi K)^2$ is the momentum conjugated to ψ [see, e.g, *Artemyev et al.*, 2013, Appendix]. The Hamiltonian (7) takes the from of classical Hamiltonian of pendulum with torque [*Arnold et al.*, 2006]. For periodical wave $F = \sin\psi$ the phase portrait of Hamiltonian (7) is shown in Figure 1a. The area of phase space filled by closed trajectories is surrounded by the separatrix. Particles moving along these trajectories are oscillating around the resonance location $\dot{\psi} = 0$ and therefore correspond to trapped particles.

Area S_{res} surrounded by the separatrix shown in Figure 1a defines the region of phase space filled by trapped particles. The equation defining S_{res} can be derived from equation (7):

$$\begin{aligned} S_{\mathrm{res}} &= \int_0^{2\pi} d\psi \int \mathrm{d}p_\psi = \oint p_\psi \mathrm{d}\psi \\ &= \frac{2^{3/2}}{\chi K}\int_{\psi_X}^{\psi_+} \sqrt{H_\psi - (\chi K)^{-1} r\psi + \phi_0 w F(\psi)}\mathrm{d}\psi \\ &= \frac{\sqrt{8\phi_0 w}}{\chi K}\int_{\psi_X}^{\psi_+} \sqrt{a\left(\psi_X - \psi\right) - F(\psi_X) + F(\psi)}\mathrm{d}\psi = \frac{\sqrt{8\phi_0 w}}{\chi K} f_s(a) \end{aligned} \tag{8}$$

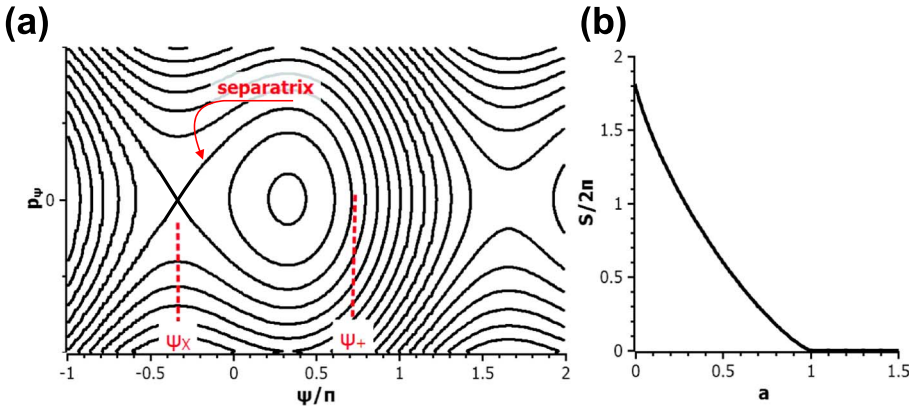

Figure 1. (a) Phase portrait of Hamiltonian system (7). (b) Profile of function $f_s(a)/2\pi$ (see equation (8)).

where $r = (\mu^* b' + (K^{-2})')/2$, $a = r/\phi_0 \chi K w$ and the saddle points ψ_X and ψ_+ are shown in Figure 1a. Area S_{res} depends on slow coordinate z and is equal to the normalized width of the resonance in p_ψ space $\Delta p_\psi = (2\pi)^{-1} \int_0^{2\pi} p_\psi d\psi = (2\pi)^{-1} S_{res}$. The Hamiltonian equation for Hamiltonian (7) shows that $p_\psi = \dot{\psi}/(K\chi)^2$. By definition we have $\dot{\psi} = \chi(Kp_z - 1)$. Thus, we can write the expression for the resonance width in p_z as follows:

$$\Delta p_z = \frac{\Delta\dot{\psi}}{\chi K} = \chi K \Delta p_\psi = \chi K \frac{S_{res}}{2\pi} = \sqrt{8\phi_0 w}\frac{f_s(a)}{2\pi}. \tag{9}$$

The profile of function $f_s(a)/2\pi$ is shown in Figure 1b. To describe the rate of energy variation of trapped particles, we substitute the resonance condition $p_z = 1/K$ into Hamiltonian (3): $H_{tr} = (\mu^* b + K^{-2})/2$. Thus, the time derivative of H_{tr} gives

$$\dot{H}_{tr} = \frac{1}{2K}\left(\mu^* b' + (K^{-2})'\right) = r/K \tag{10}$$

To obtain the average energy value of trapped particle, we perform an integration over area in the plane (ψ, p_ψ) filled by closed trajectories.

$$\left\langle \dot{H}_{tr} \right\rangle = \frac{1}{2\pi}\int_0^{2\pi} \dot{H}_{tr} d\psi \int dp_\psi \approx r\frac{S_{res}}{2\pi K} = \frac{r\Delta p_z}{\chi K^2}. \tag{11}$$

Let us consider particles moving along open (transient) trajectories in Figure 1a. In contrast to trapped particles, transient particles interact with waves for a short time interval. The corresponding rate of change of particle energy can be calculated from $\dot{H}_{ut} = \chi\phi_0 w F'$ (see equation (4)). The change of energy can be defined after integration over time:

$$\delta H_{ut} = 2\chi \int_{-\infty}^{t^*} \phi_0 w F' dt = \int_{-\infty}^{\psi^*} \frac{\sqrt{2}\chi\phi_0 w F'}{\sqrt{H_\psi - (\chi K)^{-1} r\psi + \phi_0 w F(\psi)}} d\psi \tag{12}$$

where ψ^* is the value of ψ at which the denominator of equation (12) turns to zero and t^* is the moment when $\psi = \psi^*$. The average rate of change of the transient particle energy can be calculated as multiplication of energy change (12) and phase flux of transient particles $(2\pi)^{-1} d(\int p_\psi d\psi)/dt$. *Neishtadt* [1999] derived following expression for this rate [see also *Shklyar*, 2011; *Vasko et al.*, 2016]:

$$\left\langle \dot{H}_{ut} \right\rangle = -r\frac{S_{res}}{2\pi K} = -\frac{r\Delta p_z}{\chi K^2}. \tag{13}$$

Equations (11) and (13) show that the average rates of change of the energy of transient (untrapped) and trapped particle have opposite signs. Thus, for uniformly distributed particles, contributions of transient and trapped populations totally compensate each other. This result was obtained for Langmuir waves propagating in inhomogeneous plasma [*Istomin et al.*, 1976] and whistler waves *Shklyar* [2011]. Moreover, even for localized

solitary electrostatic waves, equation $\langle H_{tr}\rangle = -\langle H_{ut}\rangle$ is satisfied [*Vasko et al.*, 2016]. This equality justifies the test particle approach for investigation of trapped particle acceleration, because accelerated particles receive energy not from waves, but from transient particles. Of course, for more realistic situations the equations for $\langle H_{tr}\rangle$ and $\langle H_{ut}\rangle$ should be rewritten for a particular electron velocity distribution [*Istomin et al.*, 1976; *Shklyar and Matsumoto*, 2009; *Shklyar*, 2011; *Vasko et al.*, 2016]. This problem is solved for KAWs in the next section and Appendix B.

3. Estimates of Electron Fluxes

To estimate the maximum level of electron flux that can be generated by acceleration of trapped particles by KAWs, we should find both the density of trapped particles n_{tr} and maximum energy $w_{tr,\max}$

$$\begin{aligned} n_{tr} &\approx \Pi \int\limits_{V_{\rm trap}} f_0 \mathrm{d}^3 v \mathrm{d}\psi \\ w_{tr}(z_{\rm esc}) &\approx \frac{\Pi}{n_{tr}} \int\limits_{V_{\rm trap}} H_{tr} f_0 \mathrm{d}^3 v \mathrm{d}\psi \end{aligned} \tag{14}$$

where f_0 is the electron distribution function in the region of KAW generation (where the main fraction of particles become trapped), $\Pi < 1$ is the probability of trapping (i.e., the ratio of number of particles which can be trapped to the actual number of trapped particles; see the definition of Π in *Arnold et al.* [2006] and *Artemyev et al.* [2015b, and references therein]), $V_{\rm trap}$ is the volume in velocity and phase ψ space filled by trapped particles, $z_{\rm esc}$ is the position where the largest fraction of trapped particles escape from the resonance. Note that the flux of trapped electrons can be estimated from $j_{tr} = n_{tr}\sqrt{w_{tr}}$.

A zeroth-order approximation of trapping acceleration can be made in which the wave amplitude is constant, i.e., under the assumption that acceleration does not lead to significant wave damping [*Artemyev et al.*, 2015a]. In this case, one can calculate $z_{\rm esc} = z_{\rm esc,max}$ from the vanishing of closed (trapped) trajectories in the phase plane (ψ, p_ψ) for Hamiltonian (7): $r(z_{\rm esc}) \approx \chi\phi_0 w(z_{\rm esc})K(z_{\rm esc})$. Solution of this equation was derived in *Artemyev et al.* [2015a]. However, this approximation provides only the maximum possible energy w_{tr} and does not limit the number of trapped particles n_{tr} (i.e., we can choose $\Pi = 1$ and accelerate all available particles). Such strong acceleration of a large amount of particles will result in rapid wave damping, which violates the assumption of constant wave amplitude. Thus, the zeroth-order approximation provides estimates for w_{tr} but cannot be used to estimate j_{tr}.

A more accurate (i.e., the first order) approximation is to assume that the waveform $\Phi(\phi)$ is not changed, but we take into account energy conservation in the system. In this case, we should compare the variations of energies of trapped particles and transient particles. When energy transferred from transient particles to the wave becomes smaller than energy transferred from the wave to trapped particles, the wave rapidly damps and trapped particles escape from the wave potential. The position at which this first occurs, $z_{\rm esc}$, depends on n_{tr} (i.e., on Π). Due to conservation of energy, a large population of trapped particles will be accelerated to lower energy than a small population. There is a minimum value of n_{tr} that corresponds to $z_{\rm esc}$ equal to $z_{\rm esc,max}$. However, the maximum j_{tr} can be reached for a larger value of n_{tr}. First-order approximation self-consistency provides $j_{tr,\max}$ and so we will determine it for two different systems: the equatorial plasma sheet and plasma sheet boundary layer.

To determine $z_{\rm esc}$, let us consider the energy variation of trapped and transient particles

$$\dot{W}_{tr} \approx \Pi \int\limits_0^{2\pi} \mathrm{d}\psi \int\limits_{V_{\rm trap}} \dot{H}_{tr} f_0 \mathrm{d}^3 v, \quad \dot{W}_{ut} \approx \int\limits_0^{2\pi} d\psi \int \dot{H}_{ut} f \mathrm{d}^3 v \tag{15}$$

where f is the local velocity distribution of resonant particles and the equality $\dot{W}_{tr} = -\dot{W}_{ut}$ defines $z_{\rm esc}$.

We provide a derivation that allows us to determine $z_{\rm esc}$ for the case of a bi-Maxwellian electron distribution, in Appendix B:

$$\dot{W}_{tr} + \dot{W}_{ut} \approx T_{e,\perp} v_{\|R} n_0 \left(\Pi G_0 - G\right) \tag{16}$$

where $T_{e,\perp}$ is the transverse component of electron temperature, n_0 is the electron density in the wave-generation region, and G is defined by equation (B8), and $v_{\|R}$ is defined by equation (A7). In the region of wave generation we have $\dot{W}_{tr} + \dot{W}_{ut} \sim (\Pi - 1) < 0$, i.e., when the energy transferred to waves from transient particles exceeds the energy transferred from waves to trapped particles. It can be shown that as z increases the contribution from transient particles decreases (as $v_{\|R}$ grows). Thus, equating the right-hand side of equation (16) to zero (i.e., equating total energy variation of transient and trapped particle to zero), we can find z_{esc} for given system parameters.

3.1. Equatorial Plasma Sheet

In this subsection we consider electron trapping and acceleration by KAWs generated in the near-Earth equatorial plasma sheet. The magnetic field can be reasonably approximated by a dipole field in this region. The corresponding spatial scale $R = R_E L$ where R_E is the Earth's radius, and $R_E L$, is the distance from the Earth to the equatorial root of magnetic field line. The plasma density distribution along the equator is described by the *Sheeley et al.* [2001] model. We use the following model parameters: wave transverse electric field amplitude $E_\perp$, transverse $T_{e,\perp}$ and parallel $T_{e,\|}$ components of electron temperature, transverse wavelength $\lambda_\perp$ in the KAW generation region (to set this parameter, we use $k_{0,\perp}\rho_i = 2\pi\rho_i/\lambda_\perp$ parameter where ρ_i is an ion gyroradius), wave frequency ω normalized by the ion gyrofrequency Ω_{0i}, ion temperature T_i, magnetic field B_0, and plasma density n_0 in the KAW generation region. Default values of these parameters are as follows: $E_\perp = 50$ mV/m, $T_{e,\perp} = 100$ eV, $T_{e,\|} = 150$ eV, $k_{0,\perp}\rho_i = 0.65$, $\omega/\Omega_{0i} = 0.5$, $T_i = 1$ keV, $B_0 = 42$ nT, and $n_0 = 1$ cm^{-3} (equatorial magnetic field and plasma density at L shell about 9). Then we fix all parameters and vary two of them in wide ranges. We should mention that some of the parameters are at the upper end of the validity of the KAW dispersion relation (e.g., ω/Ω_{0i} cannot reach one for KAWs). We use such range of ω/Ω_{0i} only to illustrate how the efficiency of trapping scales with the wave frequency.

For each set of parameters that are presented we calculate the maximum change in the electron flux Δj_{max} normalized by the initial thermal electron flux $j_0 = n_0\sqrt{2T_{e,\perp}/m_e}$ in the wave generation mechanism. Here Δj_{max} is defined as the maximum difference between j_{tr} and $j_{0,tr}$ where $j_{0,tr}$ equals to j_{tr} in the wave-generation region. Eight 2-D maps of $\Delta j_{max}/j_0$ are shown in Figure 2. This figure demonstrates that electron trapping by KAWs can transform ~5–15% of the initial thermal flux into accelerated electrons. Let us consider how $\Delta j_{max}/j_0$ depends on system parameters.

1. $(E_\perp, T_{e,\perp})$ *map*. The most intense fluxes of accelerated electrons are generated when KAWs have large amplitudes $E_\perp$ and interact with cold electrons. In both systems with $E_\perp = 10$ mV/m, $T_{e,\perp} = 10$ eV and $E_\perp = 100$ mV/m, $T_{e,\perp} = 100$ eV trapping acceleration produces $\Delta j_{max}/j_0 \sim 0.1$. For hot background electrons ($T_{e,\perp} = 300$ eV) and low-amplitude KAWs $E_\perp = 10$ mV/m the acceleration mechanism is ineffective, whereas the acceleration of cold electrons $T_{e,\perp} = 10$ eV by very intense KAWs $E_\perp = 100$ mV/m results in generation $\Delta j_{max}/j_0 \sim 0.25$.
2. $(E_\perp, k_{0,\perp}\rho_i)$ *map*. Both very long wavelength ($k_{0,\perp}\rho_i = 0.1$) and very short wavelength ($k_{0,\perp}\rho_i = 10$) KAWs are ineffective at producing electron acceleration. The strongest effects of trapping can be reached in the system with $k_{0,\perp}\rho_i \in [0.6, 3]$ and more intense KAWs.
3. $(E_\perp, \omega/\Omega_{0i})$ *map*. Higher-frequency KAWs trap and accelerate electrons more effectively, e.g., intense $E_\perp = 100$ mV/m high-frequency $\omega/\Omega_{0i} > 0.6$ KAWs can generate $\Delta j_{max}/j_0 \sim 0.1$.
4. $(E_\perp, T_i/T_{e,\perp})$ *map*. KAWs propagating in colder plasma (smaller $T_i/T_{e,\perp}$) accelerate electrons more effectively. In both systems with $E_\perp = 10$ mV/m, $T_i/T_{e,\perp} \sim 1$ and $E_\perp = 100$ mV/m, $T_i/T_{e,\perp} \sim 10$ trapping acceleration produces $\Delta j_{max}/j_0 \sim 0.05$. For $T_i/T_{e,\perp} \sim 10$ and low-amplitude KAWs $E_\perp = 10$ mV/m acceleration mechanism is ineffective, whereas the acceleration in a system with $T_i/T_{e,\perp} \sim 1$ and very intense KAWs $E_\perp = 100$ mV/m results in $\Delta j_{max}/j_0 \sim 0.1$.
5. $(T_{e,\|}, T_{e,\perp})$ *map*. In a system with transverse anisotropy $T_{e,\|}/T_{e,\perp} < 1$ the acceleration is ineffective. The largest fluxes $\Delta j_{max}/j_0 \sim 0.25$ are generated in the case of cold electrons $T_{e,\|} \sim T_{e,\perp} \sim 10$ eV. For hotter electrons $T_{e,\|} > 100$ eV the acceleration of trapped electrons can lead to $\Delta j_{max}/j_0 \sim 0.05$ independently of the anisotropy level if $T_{e,\|}/T_{e,\perp} > 1$.
6. $(\omega/\Omega_{0i}, k_{0,\perp}\rho_i)$ *map*. This map is almost identical to the $(E_\perp, k_{0,\perp}\rho_i)$ map if we assume that the ω/Ω_{0i} variation from 0.1 to 1 corresponds to $E_\perp$ variation from 10 mV/m to 100 mV/m.
7. (n_0, B_0) *map*: Stronger magnetic field and smaller plasma density ($B_0 \sim 100$ nT, $n_0 \sim 0.1$ cm^{-3}) corresponds to larger Alfvén velocity, and thus, in such a system more particles can be trapped and accelerated by KAWs ($\Delta j_{max}/j_0 \sim 0.25$). A decrease of B_0 (or/and density increase) results in a reduction of the efficiency of trapping acceleration.

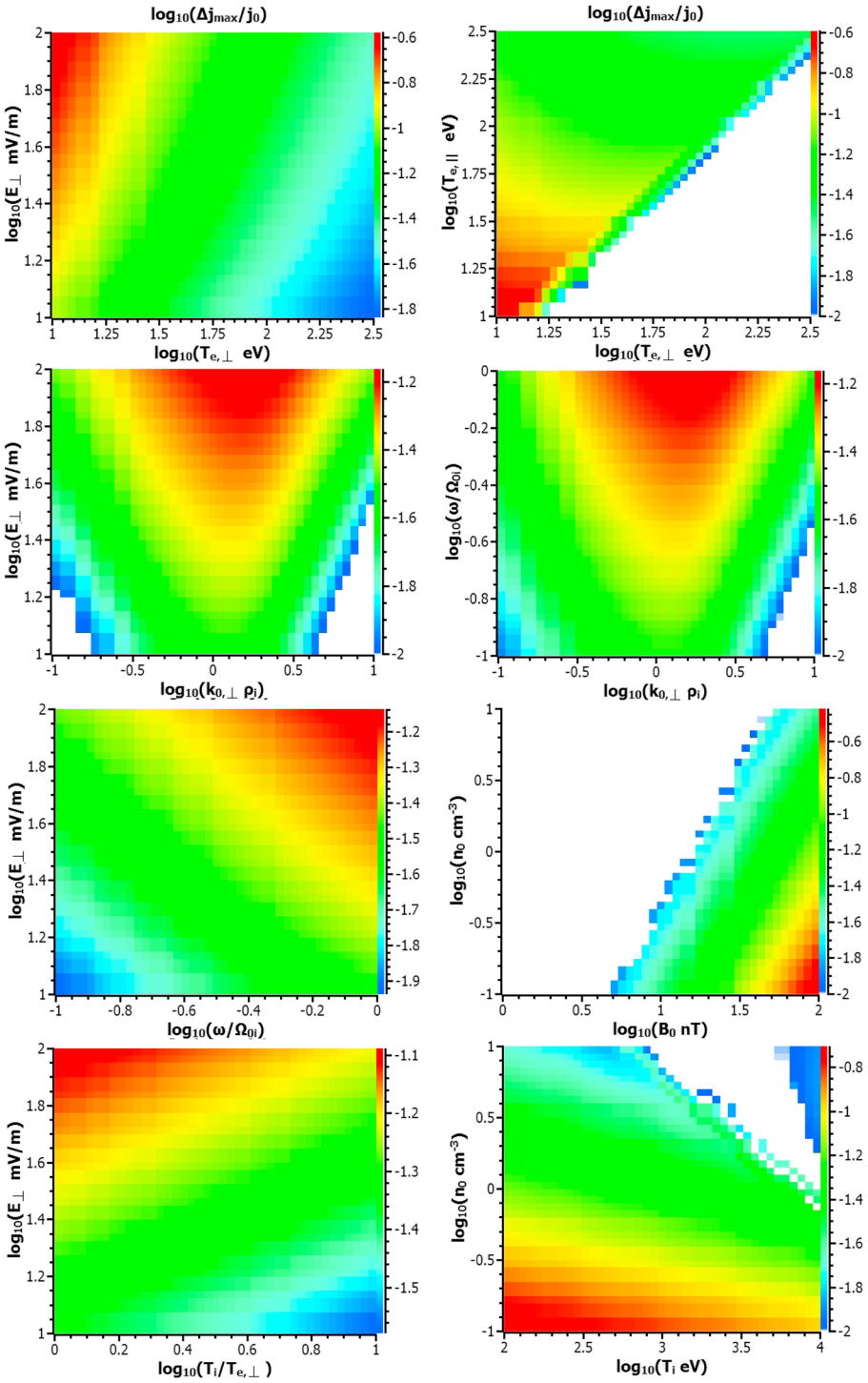

Figure 2. Maps of maximum generated flux j_{max} for equatorial magnetosphere. System parameters are listed in the text. White color shows $\Delta j_{max}/j_0 \leq 0.01$.

8. (n_0, T_i) *map*: The most effective acceleration occurs in a system with cold ions ($T_i \sim 100$ eV) and small density. Increasing T_i or n_0 results in a decrease of the efficiency of acceleration.

We can derive a general conclusion from these eight maps: in cold-enough plasma with stronger magnetic field and lower density, KAWs with higher frequency and $k_{0,\perp}\rho_i \sim 1$ can generate 10–25% of fluxes of accelerated electrons. The most effective generation of accelerated electron fluxes corresponds to high parallel

wave intensity which depends significantly on wave dispersion (see equation (A4)). Lister ranges of background plasma/magnetic field parameters and wave properties (high frequency, $k_{0,\perp}\rho_i \sim 1$) correspond to high-parallel fields for given transverse wavefield amplitude.

3.2. Plasma Sheet Boundary Layer

To model electron trapping at the boundary of the plasma sheet, we consider again a dipole magnetic field with *L* shell equal to 9 and initial latitude about 40°. The corresponding position is located around 5.5 R_E away from the ionosphere along the magnetic field line. The electron density is taken to be constant along magnetic field lines (see discussion of the corresponding plasma conditions in *Watt and Rankin* [2010]). The main system parameters and their default values are the same as in section 3.1, but the wave generation region is located around magnetic latitude $\lambda \sim 40°$ with the corresponding amplitude of the background magnetic field $B_0 \approx$ 320 nT. Figure 3 shows eight maps of fluxes of accelerated electrons $\Delta j_{max}/j_0$. Let us compare dependencies plotted in Figures 2 and 3.

1. $(E_\perp, T_{e,\perp})$ *map*. Amplitudes of KAWs sufficient for trapping and acceleration of electrons are larger in the plasma sheet boundary. KAWs with $E_\perp = 50$ mV/m can effectively accelerate only electrons with $T_{e,\perp} \in [25, 100]$ eV. To generate $\Delta j_{max}/j_0 \sim 0.25$, KAWs with $E_\perp = 100$ mV/m should interact with electron $T_{e,\perp} =$ 25 eV. In contrast to the equatorial plane, in the plasma sheet boundary the most effective acceleration is not for coldest electrons, but for some intermediate temperature.
2. $(E_\perp, k_{0,\perp}\rho_i)$ *map*. This map is similar for both systems (equatorial and boundary plasma sheets), but for boundary plasma sheet the range of parameters corresponding to inefficient acceleration and trapping is much wider.
3. $(E_\perp, \omega/\Omega_{0i})$ *map*. In contrast to equatorial plasma sheet, in the plasma sheet boundary only higher-frequency ($\omega/\Omega_{0i} > 0.3$) intense ($E_\perp > 40$ mV/m) KAWs can trap and accelerate electrons more effectively.
4. $(E_\perp, T_i/T_{e,\perp})$ *map*. This map repeats dependencies shown for the equatorial plasma sheet, but for the boundary plasma sheet the range of parameters corresponding to inefficient acceleration and trapping is much wider.
5. $(T_{e,\|}, T_{e,\perp})$ *map*. In the plasma sheet boundary the KAW interaction with transversely anisotropic electrons $T_{e,\|}/T_{e,\perp} < 1$ can result in generation $\Delta j_{max}/j_0 \sim 0.05$ (in contrast with questorial plasma sheet where such acceleration is inefficient for $T_{e,\|}/T_{e,\perp} < 1$).
6. $(\omega/\Omega_{0i}, k_{0,\perp}\rho_i)$ *map*. This map is almost identical to the $(E_\perp, k_{0,\perp}\rho_i)$ map (similar to the equatorial plasma sheet).
7. (n_0, λ) *map*. KAWs trap and accelerate electrons at lower latitudes more effective than at high latitudes. The most farovable region of KAW generation is located around $\lambda \sim 40°$ where KAWs propagating in rarified plasma $n_0 < 0.3$ cm^{-3} can generate $\Delta j_{max}/j_0 \sim 0.3$.
8. (n_0, T_i) *map*. This map is similar for both systems (equatorial and boundary plasma sheets)—the most effective acceleration corresponds to cold ions ($T_i \sim 100$ eV) and small density.

4. Discussion and Conclusions

We have considered the interesting effect where waves play the role of mediator between two populations of transient and trapped resonant particles (see more about this effect in *Shklyar and Matsumoto* [2009] and *Shklyar* [2011]). The contribution of transient electrons can overcome the energy gained by the trapped population, thus allowing KAWs to accelerate trapped particles without significant damping of the wave. This potentially explains why KAWs are widely observed in the inner magnetosphere and plasma sheet boundary [e.g., *Wygant et al.*, 2002; *Ergun et al.*, 2015; *Chaston et al.*, 2015; *Malaspina et al.*, 2015]. The energy transfer process between trapped and transient electrons allows KAWs to transport trapped particles along geomagnetic field lines to the region where the wave parallel electric field can no longer compensate the mirror force acting on trapped particles. At this escape location, trapped accelerated electrons form beams moving freely along magnetic field lines. Our analysis shows that the energy gained by trapped electrons can be estimated based on the assumption of constant wave amplitude and a test-particle approach.

The model we have used makes the assumption that all trapped electrons are captured into the effective potential well around the wave generation region where the wave amplitude grows exponentially due to, for example, instability of ion flows or transformation of hydrodynamic waves into KAWs [*Hasegawa*, 1976; *Voitenko*, 1998; *Zhao et al.*, 2011; *Chaston et al.*, 2012]. Significant wave growth may also occur as a result of

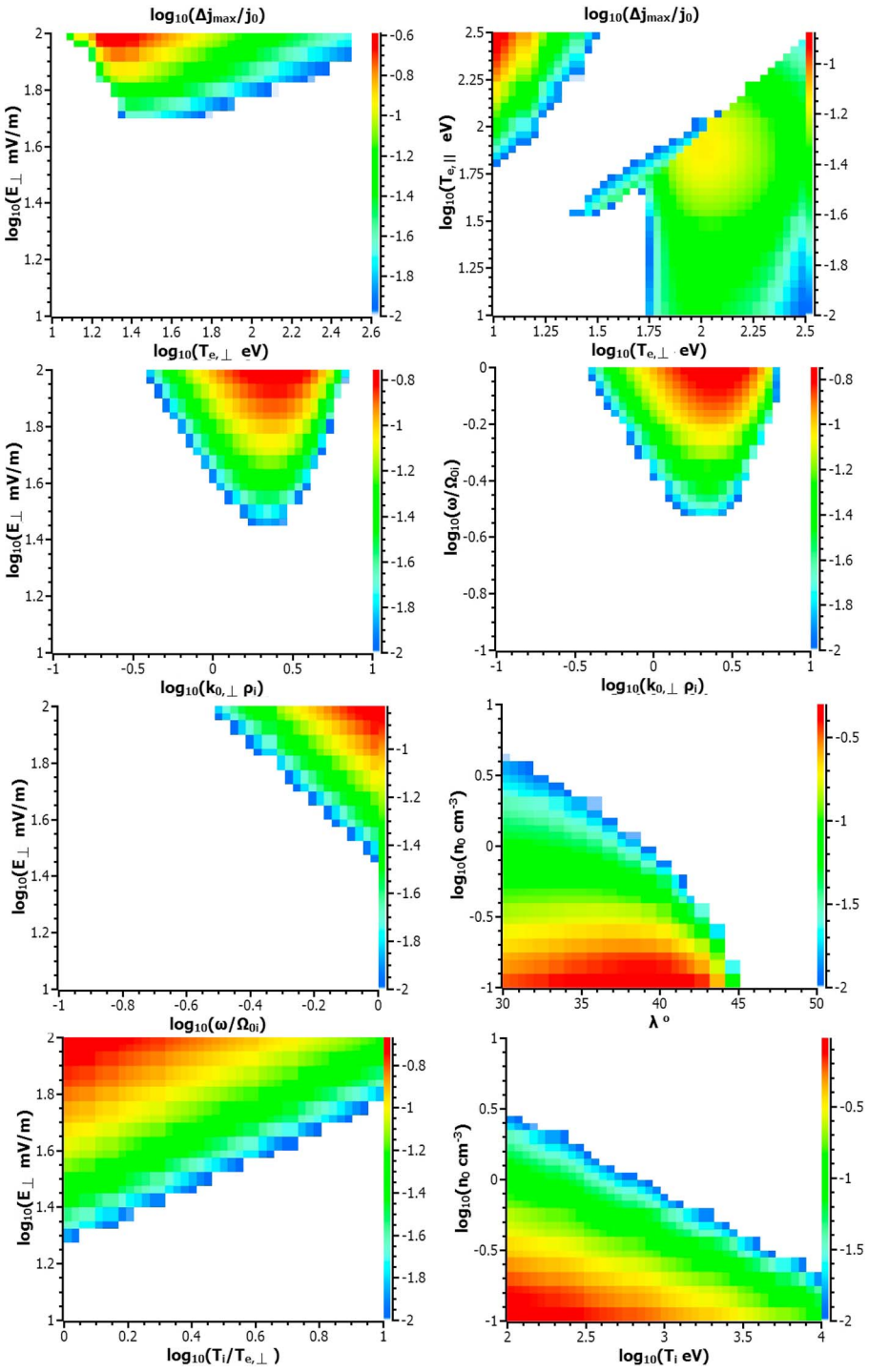

Figure 3. Maps of maximum generated flux j_{max} for plasma sheet boundary. System parameters are listed in the text. White color shows $\Delta j_{max}/j_0 \leq 0.01$.

energy transferred from transient electrons to the wave as it propagates along the geomagnetic field. This effect will allow new particles to be trapped into resonance until the contributions from transient and trapped particles compensate one another. For KAWs propagating in an inhomogeneous magnetic field, the equilibrium state where transient and trapped particle effects are compensated is reached only after waves have propagated a long distance from their generation region. Thus, KAWs propagating in an inhomogeneous magnetic field can be said to be in a state of dynamic equilibrium where energy transferred between transient and trapped particles mediates growth and damping of the wave.

To conclude, we have considered electron resonant acceleration by KAWs propagating in an inhomogeneous magnetic field. Comparing contributions of transient and trapped particles, we have found the maximum amplitudes of fluxes of electrons accelerated via trapping into resonance. For a rather wide range of system parameters, acceleration by KAWs can generate up to ~5–25% of background fluxes both in the equatorial plasma sheet and in the plasma sheet boundary. The most preferential conditions for electron acceleration correspond to cold ion and electrons, stronger background magnetic field, higher wave frequency, rarefied plasma density, and transverse wavelength about ion gyroradius.

Appendix A: Wave Models

To describe KAWs propagating in inhomogeneous magnetic field, we use dispersion relation from *Chaston et al.* [2013]:

$$k_\parallel^2 v_A^2 k_\perp^2 \rho_s^2 = \left(\omega^2 - \frac{k_\parallel^2 v_A^2}{\eta}\right)\left(1 - \frac{k_\parallel^2 v_s^2}{\omega^2}\left(1 - \eta k_\perp^2 \rho_i^2\right)\right) \tag{A1}$$

where v_A is the Alfvén velocity, $v_s = \sqrt{2T_{e,\perp}/m_i}$ is the sound speed, $\rho_s = v_s m_i c/eB$, $\rho_i = \rho_s\sqrt{T_i/T_{e,\perp}}$, T_i is the ion temperature, $T_{e,\perp}$ is the electron temperature,

$$\eta = \frac{1}{k_\perp^2 \rho_i^2}\left(1 - I_0(k_\perp^2 \rho_i^2) e^{-k_\perp^2 \rho_i^2}\right) \tag{A2}$$

and I_0 is the zeroth-order-modified Bessel function. Solving equation (A1) relative to $k_\parallel$, we obtain

$$\begin{aligned} k_\parallel &= \frac{\omega}{v_A}\sqrt{\frac{a_1 - \sqrt{a_1^2 - 4a_0}}{2a_0}} \\ a_0 &= \frac{v_s^2}{v_A^2}\frac{1}{\eta}, \quad a_1 = \frac{v_s^2}{v_A^2}\left(1 - \eta k_\perp^2 \rho_i^2\right) + \frac{1}{\eta} + k_\perp^2 \rho_s^2. \end{aligned} \tag{A3}$$

In this study we use dispersion relation (A1), which is more general than dispersion $k_\parallel v_A = \omega(k_\perp^2 \rho_s^2 + k_\perp^2 \rho_i^2)^{-1/2}$ derived by *Hasegawa* [1976]. To obtain *Hasegawa* [1976] equation from equation (A1), one should consider the limit $k_\perp \rho_i \gg 1$, when $\eta \sim (k_\perp \rho_i)^{-2}$, $a_0 \sim (k_\perp \rho_i v_s/v_A)^2$, $a_1 \sim k_\perp^2(\rho_s^2 + \rho_i^2)$, and equation (A3) takes the form $k_\parallel v_A = \omega(k_\perp^2 \rho_s^2 + k_\perp^2 \rho_i^2)^{-1/2}$.

For dispersion relation (A1) the ratio of parallel and transverse components of the wave electric field can be written as [*Chaston et al.*, 2013]

$$\frac{E_\parallel}{E_\perp} = -\frac{k_\parallel k_\perp \omega^2 \rho_s^2 \eta}{\omega^2 - k_\parallel^2 v_s^2\left(1 - k_\perp^2 \rho_i^2 \eta\right)} = \frac{k_\parallel}{k_\perp}\left(1 - \frac{\omega^2}{k_\parallel^2 v_A^2}\eta\right) = \frac{k_\parallel}{k_\perp}\left(1 - \frac{2a_0\eta}{a_1 - \sqrt{a_1^2 - 4a_0}}\right). \tag{A4}$$

In this study we use amplitude $E_\perp$ as an input parameter and recalculate $E_\parallel$ along magnetic field lines from equation (A4) with $k_\parallel$ defined by equation (A3). We also use the transverse wave number $\lambda_{0\perp}$ defined in the region of wave generation. The transverse wave number is recalculated along magnetic field lines as $k_\perp = (2\pi/\lambda_{0\perp})\sqrt{b}$ where $b = B/B_0$ [see *Watt and Rankin*, 2012, and references therein]. Ion temperature T_i is assumed to be constant along magnetic field lines. We introduce the dimensionless wave number:

$$\begin{aligned} K &= \frac{k_\parallel}{k_0} = \frac{v_{A0}k_\parallel}{\omega} = \frac{\sqrt{n}}{b}\sqrt{\frac{a_1 - \sqrt{a_1^2 - 4a_0}}{2a_0}} \\ a_0 &= \frac{T_e}{T_i}\beta\frac{n}{b}\frac{x_\perp}{1 - I_0(x_\perp)e^{-x_\perp}} \\ a_1 &= \frac{T_e}{T_i}\left(\beta\frac{n}{b}I_0(x_\perp)e^{-x_\perp} + x_\perp\right) + \frac{x_\perp}{1 - I_0(x_\perp)e^{-x_\perp}} \\ x_\perp &= \left(\frac{2\pi\rho_i}{\lambda_{\perp 0}}\right)^2\frac{1}{b} \end{aligned} \tag{A5}$$

where n is the plasma density normalized by the value n_0 in the wave generation region, $\beta = 8\pi n_0 T_i/B_0^2$. The dimensionless wave amplitude (in scalar potential) is

$$\phi_0 w = \frac{eE_\parallel}{k_\parallel m_e v_{A0}^2} = \underbrace{\frac{eE_\perp \lambda_{0\perp}}{2\pi m_e v_{A0}^2}}_{\phi_0} \underbrace{\frac{1}{\sqrt{b}}\left(1 - \frac{2a_0\eta}{a_1 - \sqrt{a_1^2 - 4a_0}}\right)}_{w}. \tag{A6}$$

The dimensional resonant velocity is

$$v_{\parallel R} = \frac{\omega}{k_\parallel} = v_{A0}\frac{b}{\sqrt{n}}\sqrt{\frac{2a_0}{a_1 - \sqrt{a_1^2 - 4a_0}}}. \tag{A7}$$

Finally, we define dimensionless parameter a for function (8):

$$a = \frac{1}{\phi_0 \chi}\frac{v_\perp^2 b' + (v_{\parallel R}^2)'}{2Kwv_{A0}^2}. \tag{A8}$$

Appendix B: Energy Balance

In the region of KAW generation we introduce the anisotropic distribution function of electrons

$$f_0 = \frac{2n_0}{v_{T\parallel} v_{T\perp}^2 \sqrt{\pi}} \bar{f}\left(\frac{v_\perp}{v_{T\perp}}, \frac{v_\parallel}{v_{T\parallel}}\right) \tag{B1}$$

where n_0 is the density in the wave generation region, $v_{T\perp} = \sqrt{2T_{e,\perp}/m_e}$ and $v_{T\parallel} = \sqrt{2T_{e,\parallel}/m_e}$ are components of thermal velocity. Function (B1) can be recalculated along magnetic field lines using conservation of energy and magnetic moment. To calculate variation rates of energy of trapped and transient (untrapped) particles, we need to perform the following integrations:

$$\begin{aligned} \dot{W}_{tr} &\approx \Pi \int_0^{2\pi} d\psi \int_0^{\infty} v_\perp dv_\perp \int_{V_{\text{trap}}} \dot{H}_{tr} f_0 dv_\parallel \\ \dot{W}_{ut} &\approx \int_0^{2\pi} d\psi \int_0^{\infty} v_\perp dv_\perp \int_{V_{\text{untrap}}} \dot{H}_{ut} f dv_\parallel \end{aligned} \tag{B2}$$

where V_{trap} is the phase volume filled by trapped trajectories and V_{untrap} is the phase volume filled by transient trajectories. In both integrals of equation (B2) the velocity distribution should be evaluated at resonance: $v_\parallel = v_{\parallel R0}$ for trapped particles and $v_\parallel = v_{\parallel R}$ for untrapped particles ($v_{\parallel R0}$ is $v_{\parallel R}$ value in the region of wave generation). Thus, we can rewrite equation (B2) as follows:

$$\begin{aligned} \dot{W}_{tr} &\approx \Pi \int_0^{\infty} v_\perp dv_\perp \int_{v_{\parallel R} - \Delta p/m_e}^{v_{\parallel R} + \Delta p/m_e} f_0 dv_\parallel \int_0^{2\pi} \dot{H}_{tr} d\psi \\ &= \Pi n_0 T_\perp v_{\parallel R} \frac{4}{v_{T\parallel} v_{T\perp}^4 \sqrt{\pi}} \int_0^{\infty} \tilde{r} v_\perp dv_\perp \int_{v_{\parallel -}(v_\perp)}^{v_{\parallel +}(v_\perp)} \bar{f}_0 dv_\parallel \\ &= \Pi n_0 T_\perp v_{\parallel R} G_0 \\ \dot{W}_{ut} &\approx v_{\parallel R} \frac{4}{v_{T\parallel} v_{T\perp}^4 \sqrt{\pi}} \int_0^{\infty} \tilde{r} v_\perp dv_\perp \int_{v_{\parallel -}(v_\perp)}^{v_{\parallel +}(v_\perp)} \bar{f} dv_\parallel = \Pi n_0 T_\perp v_{\parallel R} G \end{aligned} \tag{B3}$$

where $v_{\|\pm} = v_{\|R} \pm \Delta p(v_\perp)/m_e$ with Δp defined as

$$\Delta p = \sqrt{8e\Phi_0 m_e w}\frac{f_s(a)}{2\pi} = \Delta v_0 m_e \frac{f_s(a)}{2\pi} \tag{B4}$$

where $\Delta v_0 = 4\sqrt{e\Phi_0/2m_e}$ is the resonance width in velocity space. The dimensional form of r can be written as

$$\tilde{r} = \frac{1}{2}\left(v_\perp^2 b' + (v_{\|R}^2)'\right). \tag{B5}$$

Let us consider a normalized by n_0 Maxwellian distribution (B1) in the region where waves are generated

$$\bar{f}_0 = \exp\left(-\left(\frac{v_\perp}{v_{T\perp}}\right)^2 - \left(\frac{v_\|}{v_{T\|}}\right)^2\right). \tag{B6}$$

Then function (B6) can be recalculated for any b value [*Whipple et al.*, 1991] ($b = 1$ in the wave-generation region):

$$\bar{f} = \exp\left(-\left(\frac{v_\perp}{v_{T\perp}}\right)^2 \frac{1}{A} - \left(\frac{v_\|}{v_{T\|}}\right)^2\right)$$

$$A = \left(b^{-1} + \frac{T_\perp}{T_\|}(1 - b^{-1})\right)^{-1} \tag{B7}$$

Substituting equations (B5–B7) into equation (B3), we obtain

$$G_0 = \frac{2}{\sqrt{\pi}}\int_0^\infty e^{-x^2}\left(x^2 b' + \frac{(v_{\|R}^2)'}{v_{T\perp}^2}\right)x\mathrm{d}x \int_{y_-(x)}^{y_+(x)} e^{-y^2}\mathrm{d}y. \tag{B8}$$

$$G = \frac{2A}{\sqrt{\pi}}\int_0^\infty e^{-x^2}\left(x^2 Ab' + \frac{(v_{\|R}^2)'}{v_{T\perp}^2}\right)x\mathrm{d}x \int_{\tilde{y}_-(x)}^{\tilde{y}_+(x)} e^{-y^2}\mathrm{d}y$$

where (see equation (A8))

$$\begin{aligned} y_\pm(x) &= \frac{v_{\|R} \pm \Delta v_0 f_s(a)/2\pi}{v_{T\|}}, \quad \tilde{y}_\pm(x) = \frac{v_{\|R} \pm \Delta v_0 f_s(\tilde{a})/2\pi}{v_{T\|}} \\ a(x) &= \frac{\left(x^2 b' + v_{\|R}^2\right)'/v_{T\perp}^2}{2Kw\phi_0\chi}, \quad \tilde{a}(x) = \frac{\left(x^2 Ab' + v_{\|R}^2\right)'/v_{T\perp}^2}{2Kw\phi_0\chi}. \end{aligned} \tag{B9}$$

Finally, to estimate the particle flux generated by KAWs, we calculate both the density and energy of trapped particles:

$$\begin{aligned} n_{tr} &\approx \Pi n_0 \frac{2}{\sqrt{\pi}}\int_0^\infty e^{-x^2}x\mathrm{d}x \int_{y_-(x)}^{y_+(x)} e^{-y^2}\mathrm{d}y = \Pi n_0 Q \\ w_{tr} &\approx \frac{\Pi}{n_{tr}} n_0 T_\perp \frac{2}{\sqrt{\pi}}\int_0^\infty e^{-x^2}\left(x^2 b + \frac{v_{\|R}^2}{v_{T\perp}^2}\right)x\mathrm{d}x \int_{y_-(x)}^{y_+(x)} e^{-y^2}\mathrm{d}y = \frac{\Pi}{n_{tr}} n_0 T_\perp \tilde{Q} = T_\perp \frac{\tilde{Q}}{Q}. \end{aligned} \tag{B10}$$

Thus, the flux can be defined as $j_{tr} = n_{tr}\sqrt{2w_{tr}/m_e} = \Pi n_0 v_{T\perp}\sqrt{Q\tilde{Q}}$.

Acknowledgments
We are grateful to P. A. Damiano for useful discussion of KAW dispersion properties. R. Rankin acknowledges financial support from NSERC, the National Engineering and Research Council of Canada, and the Canadian Space Agency. All the new data used in this paper are obtained from analytical formulas provided here. Corresponding parameters are listed in the text. The work of I. Vasko was supported by Russian Foundation for Basic Research grant 15-32-21078.

References

Arnold, V. I., V. V. Kozlov, and A. I. Neishtadt (2006), *Mathematical Aspects of Classical and Celestial Mechanics, Dynamical Systems III. Encyclopedia of Mathematical Sciences*, 3rd ed., Springer, New York.

Artemyev, A., V. Krasnoselskikh, O. Agapitov, D. Mourenas, and G. Rolland (2012), Non-diffusive resonant acceleration of electrons in the radiation belts, *Phys. Plasmas*, *19*, 122901, doi:10.1063/1.4769726.

Artemyev, A. V., A. A. Vasiliev, D. Mourenas, O. Agapitov, and V. Krasnoselskikh (2013), Nonlinear electron acceleration by oblique whistler waves: Landau resonance vs. cyclotron resonance, *Phys. Plasmas*, *20*, 122901, doi:10.1063/1.4836595.
Artemyev, A. V., R. Rankin, and M. Blanco (2015a), Electron trapping and acceleration by kinetic Alfven waves in the inner magnetosphere, *J. Geophys. Res. Space Physics*, *120*, 10,305–10,316, doi:10.1002/2015JA021781.
Artemyev, A. V., A. A. Vasiliev, D. Mourenas, A. I. Neishtadt, O. V. Agapitov, and V. Krasnoselskikh (2015b), Probability of relativistic electron trapping by parallel and oblique whistler-mode waves in Earth's radiation belts, *Phys. Plasmas*, *22*(11), 112903, doi:10.1063/1.4935842.
Chaston, C. C. (2015), Magnetic reconnection in the auroral acceleration region, *Geophys. Res. Lett.*, *42*, 1646–1653, doi:10.1002/2015GL063164.
Chaston, C. C., J. W. Bonnell, L. Clausen, and V. Angelopoulos (2012), Energy transport by kinetic-scale electromagnetic waves in fast plasma sheet flows, *J. Geophys. Res.*, *117*, A09202, doi:10.1029/2012JA017863.
Chaston, C. C., Y. Yao, N. Lin, C. Salem, and G. Ueno (2013), Ion heating by broadband electromagnetic waves in the magnetosheath and across the magnetopause, *J. Geophys. Res. Space Physics*, *118*, 5579–5591, doi:10.1002/jgra.50506.
Chaston, C. C., J. W. Bonnell, C. A. Kletzing, G. B. Hospodarsky, J. R. Wygant, and C. W. Smith (2015), Broadband low-frequency electromagnetic waves in the inner magnetosphere, *J. Geophys. Res. Space Physics*, *120*, 8603–8615, doi:10.1002/2015JA021690.
Damiano, P. A., J. R. Johnson, and C. C. Chaston (2015), Ion temperature effects on magnetotail Alfvén wave propagation and electron energization, *J. Geophys. Res. Space Physics*, *120*, 5623–5632, doi:10.1002/2015JA021074.
Ergun, R. E., K. A. Goodrich, J. E. Stawarz, L. Andersson, and V. Angelopoulos (2015), Large-amplitude electric fields associated with bursty bulk flow braking in the Earth's plasma sheet, *J. Geophys. Res. Space Physics*, *120*, 1832–1844, doi:10.1002/2014JA020165.
Hasegawa, A. (1976), Particle acceleration by MHD surface wave and formation of aurora, *J. Geophys. Res.*, *81*, 5083–5090, doi:10.1029/JA081i028p05083.
Istomin, Y. N., V. I. Karpman, and D. R. Shklyar (1976), Drag effects when there is resonance interaction between particles and a Langmuir wave in an inhomogeneous plasma, *Sov. Phys. JETP*, *42*, 909–920.
Karney, C. F. F. (1978), Stochastic ion heating by a lower hybrid wave, *Phys. Fluids*, *21*, 1584–1599, doi:10.1063/1.862406.
Karpman, V. I., and D. R. Shklyar (1972), Nonlinear damping of potential monochromatic waves in an inhomogeneous plasma, *Sov. Phys. JETP*, *35*, 500.
Karpman, V. I., and D. R. Shklyar (1975), Nonlinear Landau damping in an inhomogeneous plasma, *Sov. Phys. JETP*, *40*, 53–56.
Karpman, V. I., I. N. Istomin, and D. R. Shkliar (1975), Effects of nonlinear interaction of monochromatic waves with resonant particles in the inhomogeneous plasma, *Phys. Scr.*, *11*, 278–284, doi:10.1088/0031-8949/11/5/008.
Kletzing, C. A. (1994), Electron acceleration by kinetic Alfvén waves, *J. Geophys. Res.*, *99*, 11,095–11,104, doi:10.1029/94JA00345.
Laval, G., and R. Pellat (1970), Particle acceleration by electrostatic waves propagating in an inhomogeneous plasma, *J. Geophys. Res.*, *75*, 3255–3256, doi:10.1029/JA075i016p03255.
Malaspina, D. M., S. G. Claudepierre, K. Takahashi, A. N. Jaynes, S. R. Elkington, R. E. Ergun, J. R. Wygant, G. D. Reeves, and C. A. Kletzing (2015), Kinetic Alfvén waves and particle response associated with a shock-induced, global ULF perturbation of the terrestrial magnetosphere, *Geophys. Res. Lett.*, *42*, 9203–9212, doi:10.1002/2015GL065935.
Neishtadt, A. I. (1999), Hamiltonian systems with three or more degrees of freedom, *NATO ASI Series C.*, *533*, 193–213, Kluwer Acad. Publ., Dordrecht, doi:10.1063/1.166236.
Northrop, T. G. (1963), *The Adiabatic Motion of Charged Particles*, Intersci. and John Wiley, New York-London-Sydney.
Nunn, D. (1971), Wave-particle interactions in electrostatic waves in an inhomogeneous medium, *J. Plasma Phys.*, *6*, 291, doi:10.1017/S0022377800006061.
Rankin, R., J. C. Samson, and V. T. Tikhonchuk (1999), Parallel electric fields in dispersive shear Alfvén waves in the dipolar magnetosphere, *Geophys. Res. Lett.*, *26*, 3601–3604, doi:10.1029/1999GL010715.
Sheeley, B. W., M. B. Moldwin, H. K. Rassoul, and R. R. Anderson (2001), An empirical plasmasphere and trough density model: CRRES observations, *J. Geophys. Res.*, *106*, 25,631–25,642, doi:10.1029/2000JA000286.
Shklyar, D., and H. Matsumoto (2009), Oblique whistler-mode waves in the inhomogeneous magnetospheric plasma: Resonant interactions with energetic charged particles, *Surv. Geophys.*, *30*, 55–104, doi:10.1007/s10712-009-9061-7.
Shklyar, D. R. (2011), On the nature of particle energization via resonant wave-particle interaction in the inhomogeneous magnetospheric plasma, *Ann. Geophys.*, *29*, 1179–1188, doi:10.5194/angeo-29-1179-2011.
Sivukhin, D. V. (1965), *Motion of Charged Particles in Electromagnetic Fields in the Drift Approximation*, vol. 1, pp. 1–104, Consultants Bureau, New York.
Tikhonchuk, V. T., and R. Rankin (2002), Parallel potential driven by a kinetic Alfvén wave on geomagnetic field lines, *J. Geophys. Res.*, *107*(A7), 1104, doi:10.1029/2001JA000231.
Vasko, I. Y., O. V. Agapitov, F. S. Mozer, A. V. Artemyev, and J. F. Drake (2016), Electron holes in inhomogeneous magnetic field: Electron heating and electron hole evolution, *Phys. Plasmas*, *23*(5), 052306, doi:10.1063/1.4950834.
Voitenko, Y. M. (1998), Excitation of kinetic Alfvén waves in a flaring loop, *Sol. Phys.*, *182*, 411–430, doi:10.1023/A:1005049006572.
Watt, C. E. J., and R. Rankin (2009), Electron trapping in shear Alfvén waves that power the aurora, *Phys. Rev. Lett.*, *102*(4), 045002, doi:10.1103/PhysRevLett.102.045002.
Watt, C. E. J., and R. Rankin (2010), Do magnetospheric shear Alfvén waves generate sufficient electron energy flux to power the aurora?, *J. Geophys. Res.*, *115*, A07224, doi:10.1029/2009JA015185.
Watt, C. E. J., and R. Rankin (2012), Alfvén Wave Acceleration of Auroral Electrons in Warm Magnetospheric Plasma, in *Auroral Phenomenology and Magnetospheric Processes: Earth And Other Planets, Geophys. Monogr. Ser.*, vol. 197, edited by A. Keiling et al., pp. 251–260, AGU, Washington, D. C., doi:10.1029/2011GM001171.
Whipple, E., R. Puetter, and M. Rosenberg (1991), A two-dimensional, time-dependent, near-Earth magnetotail, *Adv. Space Res.*, *11*, 133–142, doi:10.1016/0273-1177(91)90024-E.
Wygant, J. R., et al. (2002), Evidence for kinetic Alfvén waves and parallel electron energization at 4–6 R_E altitudes in the plasma sheet boundary layer, *J. Geophys. Res.*, *107*(A8), 1201, doi:10.1029/2001JA900113.
Zhao, J. S., D. J. Wu, and J. Y. Lu (2011), Kinetic Alfén waves excited by oblique magnetohydrodynamic Alfén waves in coronal holes, *Astrophys. J.*, *735*(2), 114.
Zhao, J. S., Y. Voitenko, D. J. Wu, and J. De Keyser (2014), Nonlinear generation of kinetic-scale waves by magnetohydrodynamic Alfvén waves and nonlocal spectral transport in the solar wind, *Astrophys. J.*, *785*, 139, doi:10.1088/0004-637X/785/2/139.
Zhao, J. S., Y. M. Voitenko, D. J. Wu, and M. Y. Yu (2016), Kinetic Alfvén turbulence below and above ion cyclotron frequency, *J. Geophys. Res. Space Physics*, *121*, 5–18, doi:10.1002/2015JA021959.